IMA Preprints Series (2002)

Micro- and macro-scopic models of rock fracture

Donald L. Turcotte*, William I. Newman†, and Robert Shcherbakov*

Institute for Mathematics and its Applications

Lind Hall, University of Minnesota, Minneapolis, MN 55455*, U.S.A.*

SUMMARY

The anelastic deformation of solids is often treated using continuum damage mechanics. An alternative approach to the brittle failure of a solid is provided by the discrete fiber-bundle model. Here we show that the continuum damage model can give exactly the same solution for material failure as the fiber-bundle model. We compare both models with laboratory experiments on the time dependent failure of chipboard and fiberglass. The power-law scaling obtained in both models and in the experiments is consistent with the power-law seismic activation observed prior to some earthquakes.

Key words: rock mechanics, damage, fracture, critical point, power-law scaling, self-similarity

1 INTRODUCTION

The brittle failure of a material is a complicated phenomena. For example, it can involve a single fracture propagating through an homogeneous solid. However, this is an idealized case that requires a preexisting crack or notch to concentrate the applied stress. The propagation of the fracture is not fully understood because of the complexities of the stress singularities at the crack tip (Freund 1990). In general, the initiation of fracture in a homogeneous material is a more com-

*Department of Earth and Atmospheric Sciences, Snee Hall, Cornell University, Ithaca, NY *14853*, U.S.A. E-mails: turcotte@geology.cornell.edu; roshch@geology.cornell.edu

†Departments of Earth & Space Sciences, Physics & Astronomy, and Mathematics, University of California, Los Angeles, CA *90095*, U.S.A. E-mail: win@ucla.edu

plex process. Initially microcracks appear, these cracks coalesce, and a through-going rupture results. In terms of the Earth's crust, brittle failure generally occurs on preexisting faults, and the applicable process is assumed to be friction. The fault fails when the applied shear stress exceeds that produced by a static coefficient of friction. During rupture the stress on the fault is given by the dynamic coefficient of friction. As long as the dynamic coefficient of friction is less than the static coefficient of friction, stick-slip behavior results and there are earthquakes. Many papers have considered the failure of one or more specific planar faults in a homogeneous elastic medium (Ben-Zion & Rice 1995). However, the Earth's crust is made up of faults on all scales that interact. One consequence of these interactions is the scale invariant Guttenberg-Richter frequency-magnitude relation for earthquakes. Evidently, the Earth's crust is a self-organizing complex medium.

A characteristic of brittle failure is damage. For the failure of pristine brittle materials, the damage consists of the microcracks that precede material failure. Hirata et al. (1987) have determined the distribution of acoustic emissions during the brittle fracture of a pristine rock. As the applied stress is increased, microcracks occur randomly and are uncorrelated. Once the applied stress approaches that associated with the initiation of fracture, the microcracks become correlated and satisfy a power-law (fractal) spatial distribution. The microcracks coalesce to form the through-going fracture. Similar results were found by Lockner (1993). Many authors have associated the fracture of pristine materials with a second-order critical point (Herrmann 1991).

While there are important similarities between the fracture of a pristine rock and an earthquake rupture, there are also important differences. The fracture of a pristine rock is an irreversible process. However, earthquake ruptures occur repetitively on preexisting faults and, between earthquakes, faults heal. If the Earth's crust, prior to a major earthquake, behaved like the fracture of a pristine rock, there would be a systematic increase in regional seismicity before a major earthquake. The rate of occurrence of small earthquakes in a seismogenic zone is nearly constant (Turcotte 1999). However, there is accumulating evidence that there is an increase in the number of intermediate-sized earthquakes prior to a large earthquake (Rundle et al. 2000). The repetitive nature of earthquakes, as well as their power-law scaling, have led some authors to argue that seismicity is an example of self-organized criticality (Bak & Tang 1989). It is certainly reason-

able to hypothesize that the Earth's crust is in a "damaged" state. Evidence of this damage is the continuous occurrence of small earthquakes that satisfy Guttenberg-Richter frequency-magnitude scaling.

In this paper we will consider both microscopic and continuum models of damage. We will compare both types of models with laboratory experiments and will discuss the implications for earthquake physics. The behavior of a rod of material under tension is illustrated schematically in Figure 1. Deviations from linear elasticity and the existence of damage are shown schematically. The stress σ in the rod is given as a function of the strain ϵ. In region I, linear elasticity is applicable and we have

$$\sigma = E_0 \, \epsilon \, , \tag{1.1}$$

where E_0 is the Young's modulus of the undamaged material, a constant. In region II, where there is a deviation from linear elasticity, microcracking is occurring. These microcracks weaken the material and result in acoustic emissions. For a prescribed stress σ, the strain ϵ is greater than the value given by (1.1). Accordingly, we write

$$\sigma = E_{\text{eff}} \, \epsilon \tag{1.2}$$

where E_{eff} is the effective Young's modulus—it is no longer assumed to be a constant. This relation between σ and ϵ provides the definition of E_{eff}.

A continuum approach to this process is to introduce a damage variable α so that (Kachanov 1986; Lemaitre & Chaboche 1990; Lyakhovsky et al. 1993; Lyakhovsky et al. 1997; Krajcinovic 1996)

$$E_{\text{eff}} = E_0 \, (1 - \alpha) \, . \tag{1.3}$$

The damage variable α quantifies the deviation from linear elasticity and the distribution of microcracks in the one-dimensional problem. In general $0 \leq \alpha \leq 1$. With $\alpha = 0$, linear elasticity is obtained with (1.1) valid, but when $\alpha = 1$, failure occurs. For quasistatic (slow) rupture it is appropriate to take the damage variable to be a function only of the applied stress $\alpha(\sigma)$. However, in most cases of interest the development of damage in a material is a transient process so that we have $\alpha \left[\sigma \left(t \right) , t \right]$. As illustrated in Figure 1, the failure of the brittle material occurs when

$\sigma(t_f) = \sigma_f$ ($\alpha = 1$), the failure stress. It should be emphasized that the dependence given in Figure 1 is highly idealized since the dependence on time is not illustrated.

Another approach to brittle failure is applicable to composite materials. A composite material is made up of strong fibers embedded in a relatively weak matrix. Failure of composite materials has been treated by many authors using the concept of fiber-bundles (Smith & Phoenix 1981; Curtin 1991; Newman & Phoenix 2001). The failure statistics of the individual fibers that make up the fiber-bundle are specified. The statistics can be either static or dynamic. In the static case, the probability of the failure of a fiber is specified in terms of the stress on the fiber. Failure is assumed to occur instantaneously. In the dynamic case, the statistical distribution of times to failure for the fibers are specified in terms of the stresses on the fibers (Coleman 1956, 1958). Experiments generally favor the dynamic-failure, fiber-bundle models. When stress is applied to a fiber-bundle, the fibers begin to fail. It is necessary to specify how the stress on a failed fiber is redistributed to the remaining sound fibers (Smith & Phoenix 1981). In the uniform load sharing hypothesis, the stress from a failed fiber is redistributed equally to the remaining fibers. This is a mean-field approximation. The alternative redistribution model is the local load sharing hypothesis. In this case the load on the failed fiber is redistributed to neighboring fibers. Local load sharing is applicable to strongly bonded fibrous (composite) materials whereas equal load sharing is applicable to weakly bonded fibrous materials.

The failure of a simple fiber-bundle under uniform load sharing is illustrated in Figure 2. Initially the load on the bundle F_0 is carried equally by the four fibers with $F = \frac{1}{4}F_0$. The weakest fiber fails and the load on that fiber is now carried by the surviving fibers with $F = \frac{1}{3}F_0$. The stress on each fiber increases from the original value σ_0 to $\frac{4}{3}\sigma_0$. The process of failure followed by stress redistribution continues until all fibers fail and no load can be carried. The fiber-bundle model can also be used as a simple model for friction where the fibers represent the asperities on a surface.

The primary purpose of this paper is to compare the microscopic fiber-bundle model for failure with the macroscopic damage model for failure in a simple geometry. We consider the two models for the failure of a rod under tension. The dynamic fiber-bundle model is considered assuming uniform load sharing. The rate of failure of fibers under an initial stress σ (per fiber) is specified.

As fibers fail, the stress on the remaining fibers increases leading to a catastrophic failure of the bundle. The fiber failures are equivalent to the microcracks that occur in a uniform brittle material as it is stressed to failure.

The second model we consider for the failure of a rod is the continuum damage model. A damage variable α is introduced as in (1.3). Based on thermodynamic considerations, an expression is introduced for the increase in the damage variable with time. When $\alpha = 1$, catastrophic failure of the rod occurs. This analysis was previously carried out by Ben-Zion & Lyakhovsky (2002).

We obtain solutions for two initial value problems. In the first, a constant force F_0 is applied instantaneously at $t = 0$. The time to failure t_f is determined. In the second problem we assume that the applied force $F(t)$ is increased linearly with time $F(t) \propto t$ until failure occurs. We show that the two models we consider can give identical solutions for these problems. Moreover, these solutions correspond to the constant applied force problem, when the time variable is suitably scaled. The damage variable α is given by the fraction of fibers that fail, namely N_f/N_0, where N_0 is the original number of fibers in the bundle and $N_f(t)$ is the number that have failed. A qualitative discussion of the relation between the fiber-bundle model and the continuum damage model has been given previously by Krajcinovic (1996).

A characteristic of material failure are the emergence of acoustic emission events. The acoustic emission events are generated by microcracks as the material is damaged. The microscopic fiber-bundle model can be used to obtain the predicted rate of acoustic emission events prior to material failure. The predictions are compared with the experimental observations of Guarino et al. (1998, 1999). These authors determine the rate of acoustic emission events generated during the failure of panels of chipboard and fiberglass. Their results agree with the predictions of the microscopic fiber-bundle model. We conclude by exploring the possible relevance of these models to seismic activation, and discuss the broader implications of these results.

2 FIBER-BUNDLE MODEL

We consider a rod that is made up of N_0 fibers. This rod can be thought of as a frictionless, stranded cable made up of N_0 strands. The standard approach to the dynamic time dependent failure of a

fiber-bundle is to specify an expression for the rate of failure of fibers (Coleman 1956, 1958; Newman & Phoenix 2001). The form of this breakdown rule is given by

$$\frac{d}{dt}\left[N_0 - N_f(t)\right] = -\nu(\sigma)\ \left[N_0 - N_f(t)\right]\ , \tag{2.1}$$

where $N_f(t)$ is the cumulative number of fibers that have failed at time t, $N_0 - N_f(t)$ is thus the number of unbroken fibers, and $\nu(\sigma)$ is known as the hazard rate, which is a function of the applied stress $\sigma(t)$.

We first consider the case in which a uniform strain ϵ_0 is applied to the fiber-bundle at time $t = 0$. In this case the stress on each fiber has a constant value σ_0 given by (1.1), where E_0 is the Young's modulus of a fiber. Since the stress on the fibers is constant, so is the hazard rate, yielding $\nu = \nu_0$ independent of time t. In this case (2.1) can be integrated to give

$$\frac{N_0 - N_f(t)}{N_0} = e^{-\nu_0 t}\ , \tag{2.2}$$

where the initial conditions $N_f(0) = 0$ has been used. The cumulative distribution function $p_c(t)$ that a fiber has failed at time t is given by

$$p_c(t) = \frac{N_f(t)}{N_0} = 1 - e^{-\nu_0 t}\ . \tag{2.3}$$

The total force $F(t)$ carried by the fiber-bundle at the time t is given by

$$F(t) = \left[N_0 - N_f(t)\right]\ \sigma_0\, a\ , \tag{2.4}$$

where a is the area of a fiber. Substituting (1.1) and (2.2) into (2.4) gives

$$F(t) = N_0\, a\, E_0\, \epsilon\, e^{-\nu_0 t}\ . \tag{2.5}$$

The force on the fiber-bundle decreases as fibers fail and catastrophic failure in a finite time does not occur.

We now consider the case in which a constant tensional force F_0 is applied to the fiber-bundle at time $t = 0$. This force remains constant and is redistributed uniformly as weak fibers fail among the survivors, until the bundle suffers a catastrophic failure. Detailing this process, the stress on each fiber is initially

$$\sigma_0 = \frac{F_0}{N_0\, a}\ . \tag{2.6}$$

As fibers fail, the stress on the surviving fibers increases. We assume equal load sharing—rendering this a mean field theory—so that all the remaining fibers have the same stress $\sigma(t)$. Thus, the effective stress experienced by a surviving fiber is related to the number of failed fibers $N_f(t)$ by

$$\sigma(t) = \frac{N_0}{N_0 - N_f(t)}\,\sigma_0\,. \tag{2.7}$$

In order to complete the specification of the problem, it is necessary to prescribe the dependence of the hazard rate ν on the stress σ. For engineering materials it is standard practice (Newman & Phoenix 2001) to empirically assume the power-law relation

$$\nu(t) = \nu_0\,\left[\frac{\sigma(t)}{\sigma_0}\right]^{\rho}\,, \tag{2.8}$$

where ν_0 is the hazard rate corresponding to the initial fiber stress σ_0. It is found experimentally that values of ρ are in the range 2 to 5 for various fibrous materials.

Substitution of (2.7) and (2.8) into (2.1) gives

$$\frac{d}{dt}\,[N_0 - N_f(t)] = -\frac{\nu_0\,N_0^{\rho}}{[N_0 - N_f(t)]^{\rho-1}}\,. \tag{2.9}$$

Integration with the initial condition $N_f(0) = 0$ gives

$$N_f(t) = N_0\,\left[1 - (1 - \rho\,\nu_0\,t)^{1/\rho}\right]\,. \tag{2.10}$$

Failure of a fiber-bundle occurs when $N_f(t_f) = N_0$, the time to failure t_f is given by

$$t_f = \frac{1}{\rho\,\nu_0}\,. \tag{2.11}$$

The stress in each of the remaining fibers is obtained by substituting (2.10) into (2.7) with the result

$$\sigma(t) = \frac{\sigma_0}{(1 - \rho\,\nu_0\,t)^{1/\rho}}\,. \tag{2.12}$$

We next determine the strain of the fiber-bundle as failure occurs. We make the assumption that each fiber satisfies linear elasticity until it fails, thus we can write

$$\epsilon(t) = \frac{\sigma(t)}{E_0}\,, \tag{2.13}$$

where E_0 is the Young's modulus applicable to all fibers up to failure. We assume that a microcrack in a fiber results in its failure, i.e., there is no "damage" in a fiber prior to failure. Since the stresses in the remaining fibers are equal with the value $\sigma(t)$, the strains are also equal with the value $\epsilon(t)$.

Substitution of (2.12) into (2.13) gives the strain $\epsilon(t)$ of each remaining fiber

$$\epsilon(t) = \frac{\sigma_0}{E_0} \frac{1}{(1 - \rho\,\nu_0\,t)^{1/\rho}} \,. \tag{2.14}$$

We define an effective Young's modulus $E_{\text{eff}}(t)$ for the fiber-bundle from (1.2) according to

$$E_{\text{eff}}(t) = \frac{\sigma_0}{\epsilon(t)} \,. \tag{2.15}$$

This is the Young's modulus of the bundle as a whole (including both failed and sound fibers) treated as an equivalent rod failing under tension. Substitution of (2.14) into (2.15) gives

$$E_{\text{eff}}(t) = E_0\,(1 - \rho\,\nu_0\,t)^{1/\rho} \,. \tag{2.16}$$

Using (2.11) for the time to failure t_f, we obtain

$$E_{\text{eff}}(t) = E_0 \left(1 - \frac{t}{t_f}\right)^{1/\rho} \,. \tag{2.17}$$

The effective Young's modulus $E_{\text{eff}}(t)$ decreases from its original value of $E_{\text{eff}}(0) = E_0$ to $E_{\text{eff}}(t_f) = 0$ at failure. This dependence is illustrated in Figure 3 for $\rho = 2$, 3, and 4.

Using (2.10), (2.17) can be rewritten in the form

$$E_{\text{eff}}(t) = E_0 \left[1 - \frac{N_f(t)}{N_0}\right] \,. \tag{2.18}$$

The effective Young's modulus $E_{\text{eff}}(t)$ is linearly proportional to the fraction of fibers that remain unbroken. We have obtained the time dependent failure of a fiber-bundle to which a constant force F_0 was applied at $t = 0$. We next obtain a solution to the same problem using the damage model.

3 DAMAGE MODEL

We have obtained a solution for the strain and effective Young's modulus during the failure of a fiber-bundle under a constant applied load. This was basically a microscopic model in a mean field. We now obtain a solution to the problem utilizing the macroscopic damage model. We again consider the failure of a rod under tension. A constant tensional force F_0 is applied to the rod at time $t = 0$.

The damage variable α has been defined in (1.3). Equating (1.3) and (2.18) we obtain

$$\alpha(t) = \frac{N_f(t)}{N_0} \,. \tag{3.1}$$

This definition of damage has been used previously (Krajcinovic 1996). In our analogy with the fiber-bundle model, we can interpret the macroscopic damage variable $\alpha(t)$ to be the fraction of fibers that have failed. We now determine the time history of strain in a rod using the damage model. We assume that σ_0 is the constant stress applied to the rod at $t = 0$. For the undamaged material $\alpha = 0$ and $E_{\text{eff}} = E_0$, failure occurs when $\alpha(t_f) = 1$ and $E_{\text{eff}}(t_f) = 0$. Based upon thermodynamic considerations (Lyakhovsky et al. 1997), the time evolution of the damage variable can be related to the strain $\epsilon(t)$ by

$$\frac{d\alpha(t)}{dt} = A\,\epsilon^2(t) \tag{3.2}$$

with A a constant for a constant applied stress. This expression can be regarded as the lowest order term to emerge from a series in ϵ; for large strains, higher order terms may become important. The rate of damage generation is proportional to the square of the strain in the material.

Substitution of (1.3) into (2.15) gives the strain $\epsilon(t)$ in the damaged rod

$$\epsilon(t) = \frac{\sigma_0}{E_0\,[1-\alpha(t)]}\,. \tag{3.3}$$

Combining (3.2) and (3.3) we obtain

$$\frac{d}{dt}\,[1-\alpha(t)] = -\frac{A\,\sigma_0^2}{E_0^2\,[1-\alpha(t)]^2}\,. \tag{3.4}$$

Integrating with the initial condition $\alpha(0) = 0$ we find

$$\alpha(t) = 1 - \left(1 - \frac{3A\,\sigma_0^2}{E_0^2}\,t\right)^{1/3}\,. \tag{3.5}$$

Substitution of (3.5) into (1.3) gives

$$E_{\text{eff}}(t) = E_0\,\left(1 - \frac{3A\,\sigma_0^2}{E_0^2}\,t\right)^{1/3}\,. \tag{3.6}$$

Failure occurs at the time t_f when $E_{\text{eff}}(t_f) = 0$ where $\alpha(t_f) = 1$; thus we have

$$t_f = \frac{E_0^2}{3A\,\sigma_0^2}\,. \tag{3.7}$$

Substituting (3.7) into (3.5) we find

$$\alpha(t) = 1 - \left(1 - \frac{t}{t_f}\right)^{1/3}\,. \tag{3.8}$$

We obtain the time dependence of the effective Young's modulus $E_{\text{eff}}(t)$ by substituting (3.7) into (1.3) with the result

$$E_{\text{eff}}(t) = E_0 \left(1 - \frac{t}{t_f}\right)^{1/3} . \tag{3.9}$$

A similar derivation of this result has been given by Ben-Zion & Lyakhovsky (2002). This solution for the effective Young's modulus $E_{\text{eff}}(t)$ using the damage model is identical to the solution for the effective Young's modulus obtained using the fiber-bundle model given in (2.17) if we take $\rho = 3$ in the hazard rate scaling relation (2.8). The two totally independent approaches give identical results when we take $\rho = 3$.

Assuming $\rho = 3$, we equate the time to failure t_f given in (2.11) for the fiber-bundle model to the time to failure t_f given in (3.7) for the damage model with the result

$$A = \frac{E_0^2 \, \nu_0}{\sigma_0^2} . \tag{3.10}$$

The constant A in the damage rate equation (3.2) is related to the hazard rate ν_0 defined in (2.8). With $\rho = 3$ we have $\nu_0 \propto \sigma_0^3$ from (2.8), thus we have $A \propto \sigma_0$ from (3.10).

4 GENERALIZED DAMAGE MODEL

In the last section we showed that the equal load sharing fiber-bundle model and the damage model have identical solutions if $\rho = 3$ in the hazard rate equation (2.8). Since the stress dependence of the hazard rate is solely empirical, the value $\rho = 3$ has no particular meaning. Significantly, $\rho = 3$ is typical of polycarbonate resins used in the manufacture of composite materials for which the fiber-bundle model was developed.

With $\rho = 3$, the damage variable $\alpha(t)$ is equal to the fraction of failed fibers $N_f(t)/N_0$ from (2.8). This is not the case for other values of ρ. We now introduce a generalized definition of damage through the relation

$$E_{\text{eff}}(t) = E_0 \, [1 - \alpha(t)]^{\frac{1}{\rho - 2}} . \tag{4.1}$$

When $\rho = 3$ this reduces to the standard definition of the variable given in (1.3). Since we are modelling one-dimensional behavior on a three-dimensional medium, we suggest that this generalization provides a phenomenological device for capturing the role played by the transverse dimensions.

An alternative generalization of the continuum damage theory has been given by Krajcinovic (1996, p. 477). Instead of introducing an arbitrary power into the basic definition of the damage variable as we have done in (4.1), this author introduces an arbitrary power $\epsilon^m(t)$ into the rate equation (3.2). We prefer the generalization of (1.3) as given in (4.1) since we assume that the rate of damage be proportional to an even power of the strain.

We again consider the failure of a rod under tension. Substitution of (4.1) into (2.15) gives the strain $\epsilon(t)$ in the damaged rod

$$\epsilon(t) = \frac{\sigma_0}{E_0\ [1-\alpha(t)]^{\frac{1}{\rho-2}}}\,. \tag{4.2}$$

Combining (4.2) and (3.2) we find

$$\frac{d}{dt}\,[1-\alpha(t)] = -\frac{A\,\sigma_0^2}{E_0^2\ [1-\alpha(t)]^{\frac{2}{\rho-2}}}\,. \tag{4.3}$$

Integrating with the initial condition $\alpha(0)=0$, we obtain

$$\alpha(t) = 1 - \left[1 - \frac{\rho\,A\,\sigma_0^2}{(\rho-2)\,E_0^2}\,t\right]^{\frac{\rho-2}{\rho}}\,. \tag{4.4}$$

Substitution of (4.4) into (4.1) gives

$$E_{\text{eff}}(t) = E_0\,\left[1 - \frac{\rho\,A\,\sigma_0^2}{(\rho-2)\,E_0^2}\,t\right]^{\frac{1}{\rho}}\,. \tag{4.5}$$

Failure occurs at the time t_f when $E_{\text{eff}}(t_f)=0$ ($\alpha(t_f)=1$), thus we have

$$t_f = \frac{(\rho-2)\,E_0^2}{\rho\,A\,\sigma_0^2}\,. \tag{4.6}$$

Using (4.6) and (4.4) we obtain

$$\alpha(t) = 1 - \left(1 - \frac{t}{t_f}\right)^{\frac{\rho-2}{\rho}}\,. \tag{4.7}$$

And the substitution of (4.6) into (4.5) gives (2.17), the result obtained for the fiber-bundle model. Equating the time to failure given in (2.11) and (4.6) we have

$$A = \frac{(\rho-2)\,E_0^2\,\nu_0}{\sigma_0^2}\,. \tag{4.8}$$

Using the generalized damage definition given in (4.1) we recover the full fiber-bundle solution valid for arbitrary ρ.

Comparing (2.18) with (4.1), we obtain

$$\alpha(t) = 1 - \left[1 - \frac{N_f(t)}{N_0}\right]^{\rho-2} . \tag{4.9}$$

When $\rho = 3$ this reduces to (3.1). For other values of ρ (4.9) gives the required dependence of $\alpha(t)$ on N_f/N_0. In the general case, the damage variable α is not simply proportional to the number of failed fibers as in (3.1). As suggested earlier, this may be the outcome of the interaction of microcracks in the two transverse dimensions with the longitudinal axis along which the tension is applied, thereby complexifying an otherwise one-dimensional problem

5 TIME DEPENDENT STRESS

In the above analysis we assumed that a force F_0 was applied to a rod instantaneously at $t = 0$. We showed that the fiber-bundle model with $\rho = 3$ and the damage model gave identical result. In order to confirm the generality of this correspondence, we now consider the case in which the applied stress σ_0 is a linearly increasing function of time

$$\sigma_0(t) = \beta\, t\,, \tag{5.1}$$

where β is a constant.

We first consider the fiber-bundle model. Again assuming equal load sharing so that (2.7) is applicable, from (5.1) the stress $\sigma(t)$ in the remaining unbroken fibers is given by

$$\sigma(t) = \frac{N_0}{N_0 - N_f(t)}\beta\, t\,. \tag{5.2}$$

We again assume that the hazard rate is given by

$$\nu(t) = \nu_f \left[\frac{\sigma(t)}{\sigma_0(t_f)}\right]^{\rho} , \tag{5.3}$$

where ν_f is the hazard rate at the failure stress $\sigma_0(t_f)$ which is given, from (5.1), by

$$\sigma_0(t_f) = \beta\, t_f\,, \tag{5.4}$$

where t_f is again the failure time. Substitution of (5.4) into (5.3) gives

$$\nu(t) = \nu_f \left[\frac{\sigma(t)}{\beta\, t_f}\right]^{\rho} . \tag{5.5}$$

Combining (2.1), (5.2), and (5.5) we have

$$\frac{d}{dt}\left[N_0 - N_f(t)\right] = -\nu_f \left(\frac{t}{t_f}\right)^{\rho} \frac{N_0^{\rho}}{\left[N_0 - N_f(t)\right]^{\rho-1}}\,. \tag{5.6}$$

Integrating with the initial condition $N_f(0) = 0$, we find

$$N_f(t) = N_0 \left[1 - \left(1 - \frac{\rho\, \nu_f}{\rho + 1} \frac{t^{\rho+1}}{t_f^{\rho}} \right) \right]^{\frac{1}{\rho}} \tag{5.7}$$

Failure of the fiber-bundle occurs when $N_f(t_f) = N_0$, the time to failure is given by

$$t_f = \frac{\rho + 1}{\rho\, \nu_f} \,. \tag{5.8}$$

Comparison of (5.8) with (2.11) shows that the time to failure for a linearly increasing stress is $\rho + 1$ times the time to failure for a constant stress. The hazards rates ν_0 in (2.11) and ν_f in (5.8) are equivalent since both apply at the time of failure.

Substitution of (5.8) into (5.7) gives

$$N_f(t) = N_0 \left\{ 1 - \left[1 - \left(\frac{t}{t_f} \right)^{\rho+1} \right] \right\}^{\frac{1}{\rho}} \,. \tag{5.9}$$

Combining (5.2), (5.4) and (5.9) we obtain

$$\sigma(t) = \sigma_0(t_f) \frac{\frac{t}{t_f}}{\left[1 - \left(\frac{t}{t_f} \right)^{\rho+1} \right]^{\frac{1}{\rho}}} \,. \tag{5.10}$$

Substitution of (5.10) into (2.13) gives the strain $\epsilon(t)$ of each remaining fiber

$$\epsilon(t) = \sigma_0(t_f) \frac{\frac{t}{t_f}}{E_0 \left[1 - \left(\frac{t}{t_f} \right)^{\rho+1} \right]^{1/\rho}} \,. \tag{5.11}$$

And the effective Young's modulus for the fiber-bundle is obtained by substituting (5.11) into (2.15)

$$E_{\text{eff}}(t) = E_0 \left[1 - \left(\frac{t}{t_f} \right)^{\rho+1} \right]^{1/\rho} \,. \tag{5.12}$$

Substitution of (5.9) into (5.12) again gives (2.18). As in (2.17), the effective Young's modulus $E_{\text{eff}}(t)$ decreases from its original value of $E_{\text{eff}}(0) = E_0$ to $E_{\text{eff}}(0) = 0$ at failure. This dependence is illustrated in Figure 4 for $\rho = 2$, 3, and 4. A comparison with Figure 3 shows that damage develops much later when σ increases linearly in time than when it is instantaneously applied.

We now consider the damage model with an applied stress that increases linearly in time. From (5.1) and (5.4) we have for $t \le t_f$

$$\sigma_0(t) = \sigma_0(t_f) \frac{t}{t_f} \,. \tag{5.13}$$

For a constant applied stress σ_0 the damage parameter A defined in (3.2) is a constant. The dependence of A on hazard rate ν_0 and σ_0 has been given in (3.10). For an applied stress that increases linearly with time we replace σ_0 in (3.10) with $\sigma_0(t)$ as given by (5.13). Further, we replace ν_0 in (3.10) with $\nu_0(t)$ which we obtain from (5.3) taking $\rho = 3$ and assuming $\nu_0(t)$ is the damage rate at stress $\sigma_0(t)$. With these substitutions (3.10) becomes

$$A(t) = \frac{E_0^2\,\nu_0(t)}{\sigma_0^2(t)} = \frac{E_0^2\,\nu_f}{\sigma_0^2(t)}\left[\frac{\sigma_0(t)}{\sigma_0(t_f)}\right]^3 = \frac{E_0^2\,\nu_f}{\sigma_0^2(t_f)}\frac{t}{t_f}\,. \tag{5.14}$$

Substitution of (5.14) into (3.2) gives

$$\frac{d\alpha(t)}{dt} = \frac{\nu_f\,E_0^2}{\sigma_0^2(t_f)}\,\frac{t}{t_f}\,\epsilon^2(t)\,. \tag{5.15}$$

And the substitution of (5.13) into (3.3) gives

$$\epsilon(t) = \frac{\sigma_0(t_f)\,t}{t_f\,E_0\,\left[1-\alpha(t)\right]}\,. \tag{5.16}$$

Using (5.16), we are able to rewrite (5.15) as follows

$$\frac{d\alpha(t)}{dt} = \frac{\nu_f}{\left[1-\alpha(t)\right]^2}\left(\frac{t}{t_f}\right)^3\,. \tag{5.17}$$

Integrating with the initial condition $\alpha(0) = 0$ we obtain

$$\alpha(t) = 1 - \left(1 - \frac{3\nu_f\,t^4}{4t_f^3}\right)^{1/3}\,. \tag{5.18}$$

Failure occurs when $\alpha(t_f) = 1$ so that

$$t_f = \frac{4}{3\nu_f}\,. \tag{5.19}$$

Combining (1.3), (5.18), and (5.19) we get

$$E_{\rm eff}(t) = E_0\,\left[1 - \left(\frac{t}{t_f}\right)^4\right]^{1/3} \tag{5.20}$$

If we take $\rho = 3$ we find (5.19) is identical to (5.8) and that (5.20) is identical to (3.9). Once again, we find that the fiber-bundle model and the damage model give identical results if $\rho = 3$. Thus, we see that the time-dependent stress model is a rescaled version of the constant stress model.

6 ACOUSTIC EMISSION EVENTS

A characteristic of materials experiencing "damage" are acoustic emission events. For a solid material stressed beyond its elastic limit the acoustic emission events are associated with microcracks.

For a fibrous material the acoustic emission events are associated with the failure of one or more fibers.

We now obtain an expression for the energy flux associated with the acoustic emission events from a fiber-bundle as fibers break using the model considered above. In our fiber-bundle model we assume that individual fibers satisfy linear elasticity until failure. Thus the stored elastic energy in a single fiber $e_f(t)$ at the time of failure is given by

$$e_f(t) = \frac{1}{2}\, V_f\, E_0\, \epsilon^2(t)\,, \tag{6.1}$$

where V_f is the volume of the fiber, E_0 is the Young's modulus of the fiber, and ϵ is the strain in the fiber given by (2.14). We assume that when a fiber fails, a fraction η_a of the stored elastic energy given by (6.1) is the energy in the acoustic emission event. The efficiency η_a is analogous to the seismic efficiency η_s, the fraction of the stored elastic energy lost during an earthquake that is radiated in the seismic waves generated by earthquake. In both earthquakes and in acoustic emission events from damaged materials, energy is also used to rupture material and in some cases is dissipated in frictional heating. We assume that the acoustic emission efficiency η_a is a constant.

The rate at which energy is lost by acoustic emission events is given by

$$\frac{de_{fa}(t)}{dt} = \eta_a\, e_f(t)\, \frac{dN_f(t)}{dt}\,, \tag{6.2}$$

where $e_{fa}(t)$ is the energy associated with the acoustic emission event and $e_f(t)$ is the stored elastic energy in a fiber. Substituting (6.1) into (6.2) we obtain

$$\frac{de_{fa}(t)}{dt} = \frac{1}{2}\, \eta_a\, V_f\, E_0\, \epsilon^2(t)\, \frac{dN_f(t)}{dt}\,. \tag{6.3}$$

Since the total volume of fibers is $N_0 V_f$, the rate of energy loss in acoustic emission events per unit volume of material $e_a(t)$ is given by

$$\frac{de_a(t)}{dt} = \frac{1}{2}\, \eta_a\, \frac{E_0\, \epsilon^2(t)}{N_0}\, \frac{dN_f(t)}{dt}\,. \tag{6.4}$$

From (2.9), the rate at which fibers fail can be written

$$\frac{dN_f(t)}{dt} = \frac{\nu_0\, N_0^\rho}{[N_0 - N_f(t)]^{\rho-1}} \tag{6.5}$$

and, from (2.10) and (2.14), we have the fiber strain at its time of failure t

$$\epsilon(t) = \frac{\sigma_0}{E_0}\left[\frac{N_0}{N_0 - N_f(t)}\right] . \tag{6.6}$$

Using (6.5) and (6.6), we can rewrite (6.4) in the form

$$\frac{de_a(t)}{dt} = \frac{1}{2}\,\eta_a\,\frac{\nu_0\,\sigma_0^2}{E_0}\,\left[\frac{N_0}{N_0 - N_f(t)}\right]^{\rho+1} . \tag{6.7}$$

Combining (2.10), (2.11), and (6.7) we obtain

$$\frac{de_a(t)}{dt} = \frac{\eta_a\,\nu_0\,\sigma_0^2}{2E_0}\,\frac{1}{\left(1 - \frac{t}{t_f}\right)^{\frac{\rho+1}{\rho}}} . \tag{6.8}$$

This is the rate at which energy is radiated in acoustic emission events during the failure of a fiber-bundle.

While the rate at which energy is lost in acoustic emission events can be determined from the microscopic fiber-bundle model, this is not the case for the macroscopic damage model. We now use our analogy between the two models to determine a relationship between the energy addition associated with damage and the loss due to acoustic emission events.

We use the damage model to determine the rate at which work is being done on a rod. Since the stress on the rod σ_0 is constant we have

$$\frac{dw(t)}{dt} = \sigma_0\,\frac{d\epsilon(t)}{dt} , \tag{6.9}$$

where $w(t)$ is the work per unit volume done on the rod. Taking the derivative of (3.3) we obtain

$$\frac{d\epsilon(t)}{dt} = \frac{\sigma_0}{E_0\,\left[1 - \alpha(t)\right]^2}\,\frac{d\alpha(t)}{dt} . \tag{6.10}$$

Substitution of (3.2), (3.3) and (6.10) into (6.9) gives

$$\frac{dw(t)}{dt} = \frac{A\,\sigma_0^4}{E_0^3\,\left[1 - \alpha(t)\right]^4} . \tag{6.11}$$

Upon substitution of (3.8) and (3.10) into (6.11) we have

$$\frac{dw(t)}{dt} = \frac{\nu_0\,\sigma_0^2}{E_0}\,\frac{1}{\left(1 - \frac{t}{t_f}\right)^{4/3}} . \tag{6.12}$$

This result was previously obtained by Ben-Zion and Lyakhovsky (2002). Comparing (6.12) with (6.8), noting that $\rho = 3$ in our analogy, we find that

$$\frac{de_a(t)}{dt} = \frac{\eta_a}{2}\,\frac{dw(t)}{dt} . \tag{6.13}$$

If the acoustic efficiency is $\eta_a = 1$, we find that one-half of the energy that is added to the damaged medium is lost in acoustic emission events.

We next determine the energy in acoustic emission when the applied stress is increasing linearly in time as given by (5.1). Combining (5.6), (6.4), and (6.6), we obtain

$$\frac{de_a(t)}{dt} = \frac{\eta_a \, \nu_f \, \sigma_0^2}{2E_0} \left(\frac{t}{t_f}\right)^{\rho} \left[\frac{N_0}{N_0 - N_f(t)}\right]^{\rho+1} . \tag{6.14}$$

Using (5.9) one obtains

$$\frac{de_a(t)}{dt} = \frac{\eta_a \, \nu_f \, \sigma_0^2}{2E_0} \left(\frac{t}{t_f}\right)^{\rho} \frac{1}{\left[1 - \left(\frac{t}{t_f}\right)^{\rho+1}\right]^{\frac{\rho+1}{\rho}}} . \tag{6.15}$$

In the vicinity of rupture, we have $(1 - t/t_f) \ll 1$. In this limit, we obtain from (6.15) that

$$\frac{de_a(t)}{dt} \propto \frac{1}{\left(1 - \frac{t}{t_f}\right)^{\frac{\rho+1}{\rho}}} . \tag{6.16}$$

Thus, the scaling in the vicinity of rupture is the same as that obtained for the constant pressure result given in (6.8).

We now compare the predicted acoustic emission associated with material failure with experiments. Guarino et al. (1998, 1999) studied the failure of circular panels (220 mm diameter, 3-5 mm thickness) of chipboard and fiberglass. A differential pressure was applied across the panels until they failed. Acoustic emission events were carefully monitored. For these relatively thin panels, bending stresses were negligible and the panels failed under tension (a mode I fracture). The acoustic emission events were used to locate the associated microcracks. Initially, the microcracks appeared to be randomly distributed across the panel. As the pressure difference was increased, the microcracks localized in the region where the final rupture occurred. In the first series of experiments given by Guarino et al. (1998) the applied pressure difference (differential stress) was increased linearly with time in accordance with (5.11).

These authors determined the cumulative energy associated with acoustic emission events prior to rupture. The observed dependence of $e_a/e_{\rm tot}$ on $(1 - t/t_f)$ is given in Figure 5a where e_a is the cumulative acoustic energy at time t and $e_{\rm tot}$ is the total acoustic energy at rupture ($t = t_f$). Clear power-law behavior is observed for $(1 - t/t_f)$ less than about 0.1. The slope is $e_a \propto (1 - t/t_f)^{-0.27 \pm 0.05}$. This is equivalent to having $de_a/dt \propto (1 - t/t_f)^{-1.27 \pm 0.05}$. This result is

in agreement with the predicted dependence given in (6.16) if we take $\rho = 3.7$. Similar results were obtained by Johansen & Sornette (2000) who studied the failure of spherical tanks of kevlar wrapped around thin metallic liners. For several runs they found $e_a \propto (1 - t/t_f)^{-1}$.

Guarino et al. (1998) also obtained an histogram for the frequency-magnitude statistics of the acoustic emission events. For the chipboard panels they found that the number of events dN/de_a with a given energy e_a satisfies the relation

$$\frac{dN}{de_a} \propto e_a^{-\gamma} \tag{6.17}$$

with $\gamma = 1.51 \pm 0.05$. For earthquakes, we have $\gamma \approx 5/3$. A similar power-law distribution has also been found to be applicable for the fiber-bundles (Hemmer & Hansen 1992; Kloster et al. 1997).

Guarino et al. (1999) carried out a second series of experiments in which the applied pressure difference across the panel was increased instantaneously to a prescribed value and was held at that value until the circular panel failed. The cumulative energy associated with acoustic emission events prior to rupture was determined. The observed dependence of $e_a/e_{\rm tot}$ on $(1-t/t_f)$ for these experiments is given in Figure 5b. Again a clear power-law behavior is observed for $(1 - t/t_f)$ less than about 0.5. Again the slope is $e_a \propto (1 - t/t_f)^{-0.27}$ which is equivalent to $de_a/dt \propto (1 - t/t_f)^{-1.27}$. This result is in agreement with the predicted dependence given in (6.8) taking $\rho = 3.7$. The experiments find the same power-law behavior for a constant applied pressure difference and for a pressure difference that is increasing linearly in time. This correspondence was also found in our analysis since the power-law dependence in (6.8) is the same as the power-law dependence in (6.16).

Although there is a scaling region in the acoustic emission data that is in accord with our analysis, there are some aspects of the data that disagree with our analysis. The cumulative acoustic emission energy can be obtained by integrating (6.8). This result is not in agreement with the experimental data given in Figure 5b for small times. We attribute this disagreement to the transition from random emission events at small times to self-organizing events as rupture is approached. Our analysis correctly predicts the self-similar scaling region near rupture.

7 SEISMIC ACTIVATION

Systematic increases in the intermediate level of seismicity prior to large earthquakes have been proposed by several authors (Sykes & Jaumé 1990; Knopoff et al. 1996; Jaumé & Sykes 1999). It has also been observed that there is a power-law increase in seismic activity prior to major earthquake. This was first proposed by Bufe & Varnes (1993). They considered the cumulative Benioff strain in a region defined as

$$\epsilon_{\rm B}(t) = \sum_{i=1}^{N(t)} \sqrt{E_i}\,, \tag{7.1}$$

where E_i is the seismic energy release in the ith precursory earthquake and $N(t)$ is the number of precursory earthquakes considered up to time t. Bowman et al. (1998) carried out a systematic study of the optimal spatial region and magnitude range to obtain power-law activation. Four examples of their results are given in Figure 6. In each case $\epsilon_B(t)$ has been correlated with the relation

$$\epsilon_{\rm B}(t) = \epsilon_{\rm Bf} - B\left(1 - \frac{t}{t_f}\right)^s\,, \tag{7.2}$$

where $\epsilon_{\rm Bf}$ is the cumulative Benioff strain when the large earthquake occurs, t_f is the time since the last large earthquake, and B is a constant. For the four earthquakes illustrated in Figure 6 it is found that $s = 0.30$ (Kern County), $s = 0.18$ (Landers), $s = 0.28$ (Loma Prieta), and $s = 0.18$ (Coalinga). Other examples of power-law seismic activation have been given by Buffe et al. (1994), Varnes and Bufe (1996), Brehm and Braile (1998, 1999), Robinson (2001), and Zöller et al. (2001).

We next extend our acoustic emission analysis to determine whether it is consistent with seismic activation. Using (6.8), the rate of the Benioff strain associated with the fiber-bundle model is given by

$$\frac{d\epsilon_{\rm B}(t)}{dt} = \sqrt{\frac{de_a(t)}{dt}} = \sqrt{\frac{\eta_a\,\nu_0}{2E_0}}\frac{\sigma_0}{\left(1 - \frac{t}{t_f}\right)^{\frac{\rho+1}{2\rho}}}\,. \tag{7.3}$$

The cumulative Benioff strain is given by

$$\epsilon_{\rm B}(t) = \epsilon_{\rm Bf} - \int_{\epsilon_{\rm B}(t)}^{\epsilon_{\rm Bf}} d\epsilon = \epsilon_{\rm Bf} - \int_t^{t_f} \frac{d\epsilon_{\rm B}(t)}{dt}\,dt\,. \tag{7.4}$$

Substituting (7.3) into (7.4) and integrating, we obtain

$$\epsilon_{\rm B}(t) = \epsilon_{\rm Bf} - \frac{\sigma_0\,(\rho-1)}{2\rho}\sqrt{\frac{\eta_a\,\nu_0}{2E_0}}\left(1-\frac{t}{t_f}\right)^{\frac{\rho-1}{2\rho}}. \tag{7.5}$$

Comparing (7.5) with (7.2), we see that the two equations are identical. Rundle et al. (2000) found that the distribution of values for the power-law exponent for 12 earthquakes was $s = 0.26 \pm 0.15$. Comparing (7.5) with (7.2), $s = 0.26$ corresponds to $\rho = 2.1$. For $\rho = 3$ we find $s = 1/3$, this result was previously obtained by Ben-Zion & Lyakhovsky (2002).

8 DISCUSSION

Anelastic deformation of solids in engineering materials is often treated using continuum damage mechanics models. At the same time, statistical physicists have developed a variety of discrete models for material failure. In this paper, we show that two widely used models, a continuum, macroscopic damage model and a discrete, microscopic fiber-bundle model, yield identical solutions for a simple rupture problem.

The fiber-bundle model we consider is the dynamic time-to-failure model with uniform load sharing. The hazard rate defined in (2.8) has a power-law dependence on stress $\sigma(t)$ with exponent ρ. We consider the failure of a rod of material under tension. We consider two cases: (1) A constant tensional load is applied to the rod instantaneously and (2) the load increases linearly with time from zero. The solutions obtained using the continuum damage model are identical to the solutions obtained using the discrete fiber-bundle model if the stress exponent $\rho = 3$. We have generalized the damage model so that solutions agree with the fiber-bundle model for arbitrary values of ρ.

Guarino et al. (1998, 1999) studied the failure of circular panels of chipboard and fiberglass. They found that the cumulative energy associated with acoustic emission events had a power-law dependence on the time to failure. We have shown that this dependence is in agreement with our solutions taking the power-law exponent $\rho = 3.7$. The power-law increase in acoustic emission is also consistent with the power-law increase in cumulative Benioff strain that has been recognized prior to a number of earthquakes (Bufe & Varnes 1993; Bowman et al. 1998).

The results given here raise a number of interesting questions regarding earthquake physics. The damage and fiber-bundle models considered in this paper yield results that are very analogous

to a second-order phase change. The power-law scaling is a characteristic of the approach to a phase change. However, material failure is a catastrophic event and is certainly not reversible. Phase changes involve a tuning parameter such as temperature or magnetic field.

Rundle et al. (2000) previously considered precursory seismic activation in terms of a self-organizing spinodal behavior. A typical first-order phase change is the boiling of water. Ordinarily water at a specified temperature is heated at the boiling temperature and water is transformed to steam at this temperature as heat is added. This is an equilibrium process. However, it is possible to superheat water into the spinodal region of the phase plane. This superheated water is metastable and time dependent boiling will occur. We suggest that the nonequilibrium irreversible boiling of water is analogous to the time dependent failure considered in this paper. Rundle et al. (2000) obtained a power-law scaling of seismic activation using spinodal theory very similar to the scaling given above.

ACKNOWLEDGMENT

The authors would like to thank Yehuda Ben-Zion, Charlie Sammis, John Rundle, Bill Klein, and Leigh Phoenix for many valuable and stimulating discussions. We take this opportunity to thank the National Science Foundation, whose financial support of the IMA programs made this collaborative research possible.

REFERENCES

Bak, P., & Tang, C., 1989. Earthquakes as a self-organized critical phenomenon, *J. Geophys. Res.,* **94**, 15,635-15,637.

Ben-Zion, Y., & Lyakhovsky, V., 2002. Accelerated seismic release and related aspects of seismicity patterns on earthquakes faults, *Pure Appl. Geophys.,* in press.

Ben-Zion, Y. & Rice, J. R., 1995. Slip patterns and earthquake populations along different classes of faults in elastic solids, *J. Geophys. Res.*, **100**, 12,959-12,983.

Bowman, D. D., Ouillon, G., Sammis, C. G., Sornette, A., & Sornette, D., 1998. An observational test of the critical earthquake concept, *J. Geophys. Res.,* **103**, 24,359-24,372.

Brehm, D. J., & Braile, L. W., 1998. Intermediate-term earthquake prediction using precursory events in the New Madrid seismic zone, *Bull. Seism. Soc. Am.,* **88**, 564-580.

Brehm, D. J., & Braile, L. W., 1998. Intermediate-term earthquake prediction using the modified time-to-failure method in Southern California, *Bull. Seism. Soc. Am.*, **89**, 275-293.

Bufe, C. G., Nishenko, S. P., & Varnes, D. J., 1994. Seismicity trends and potential for large earthquakes in the Alaska-Aleutian region, *Pure Appl. Geophys.*,**142**, 83-99.

Bufe, C. G., & Varnes, D. J., 1993. Predictive modeling of the seismic cycle of the greater San Francisco Bay region, *J. Geophys. Res.*, **98**, 9871-9883.

Coleman, B. D., 1956. Time dependence of mechanical breakdown phenomena, *J. Ap. Phys.*, **27**, 862-866.

Coleman, B. D., 1958. Statistics and time dependence of mechanical breakdown in fibers, *J. Ap. Phys.*, **29**, 968-983.

Curtin, W. A., 1991. Theory of mechanical properties of ceramic-matrix composites, *J. Am. Ceram. Soc.*, **74**, 2837-2845.

Freund, L. B., 1990. *Dynamic Fracture Mechanics*, Cambridge University Press, Cambridge.

Guarino, A., Garcimartin, A., & Ciliberto, S., 1998. An experimental test of the critical behavior of fracture precursors, *Eur. Phys. J.*, **B6**, 13-24.

Guarino, A., Ciliberto, S., & Garcimartin, A., 1999. Failure time and microcrack nucleation, *Europhys. Lett.*, **47**, 456.

Hemmer, P. C., & Hansen, A., 1992. The distribution of simultaneous fiber failures in fiber-bundles, *J. Ap. Mech.*, **59**, 909-914.

Herrmann, H. J., 1991. Fractures, in *Fractals and Disordered Systems*, A. Bundle and S. Havlin, eds., pp. 175-205, Springer-Verlag, Berlin.

Hirata, T., Satoh, T., & Ito, K., 1987. Fractal structure of spatial distribution of microfracturing in rock, *Geophys. J. Roy. Astron. Soc.*, **90**, 369-374.

Jaumé, S. C., & Sykes, L. R., 1999. Evolving towards a critical point: A review of accelerating seismic moment/energy release prior to large and great earthquakes, *Pure Appl. Geophys.*,**155**, 279-306.

Johansen, A., & Sornette, D., 2000. Critical ruptures, *Eur. Phys. J.*, **B18**, 163-181.

Kachanov, L. M., 1986. *Introduction to Continuum Damage Mechanics*, Martinus Nijhoff, Dordrecht, Netherlands.

Kloster, M., Hansen, A., & Hemmer, P. C., 1997. Burst avalanches in solvable models of fibrous materials, *Phys. Rev.*, **E56**, 2615-2625.

Knopoff, L., Levshina, T., Keilis-Borok, V. I., & Mattoni, C., 1996. Increased long-range intermediate-magnitude earthquake activity prior to strong earthquakes in California, *J. Geophys. Res.*, **101**, 5779-5796.

Krajcinovic, D., 1996. *Damage Mechanics*, Elsevier, Amsterdam.

Lemaitre, J., & Chaboche, J.-L., 1990. *Mechanics of Solid Materials*, Cambridge University Press, Cambridge.

Lockner, D. A., 1993. The role of acoustic emissions in the study of rock fracture, *Int. J. Rock Mech. Min. Sci. and Geomech. Abs.*, **7**, 883-889.

Lyakhovsky, V., Ben-Zion, Y., & Agnon, A., 1997. Distributed damage, faulting and friction, *J. Geophys. Res.*, **102**, 27,635-27,649.

Lyakhovsky, V., Podladchikov, Y., & Poliakov, A., 1993. A rheological model of a fractured solid, *Tectonophysics*, **226**, 187-198 (1993).

Newman, W. I., & Phoenix, S. L., 2001. Time dependent fiber-bundles with local load sharing, *Phys. Rev.*, **E63**, 021507.

Robinson, R., 2000. A test of the precursory accelerating moment release model on some recent New Zeland earthquakes, *Geophys. J. Int.*, **140**, 568-576.

Rundle, J. B., Klein, W., Turcotte, D. L., & Malamud, B. D., 2000. Precursory seismic activation and critical point phenomena, *Pure Appl. Geophys.*,**157**, 2165-2182.

Smith, R. L., & Phoenix, S. L., 1981. Asymptotic distributions for the failure of fibrous materials under series-parallel structure and equal load-sharing, *J. Ap. Mech.*, **48** 75-82.

Sykes, L. R., & Jaumé, S. C., 1990. Seismic activity on neighboring faults as a long-term precursor to large earthquakes in the San Francisco Bay region, *Nature*, **348**, 595-599.

Turcotte, D. L., 1999, Seismicity and self-organized criticality, *Phys. Earth. Planet. Int.*, **111**, 275-293.

Varnes, D. J., & Bufe, C. G., 1996. The cyclic and fractal seismic series preceding an m_b 4.8 earthquake on 1980 February 14 near the Virgin Islands, *Geophys. J. Int.*, **124**, 149-158.

Zöller, G., Hainzl, S., & Kurths, J., 2001. Observation of growing correlation length as an indicator for critical point behavior prior to large earthquakes, *J. Geophys. Res.*, **106**, 2167-2175.

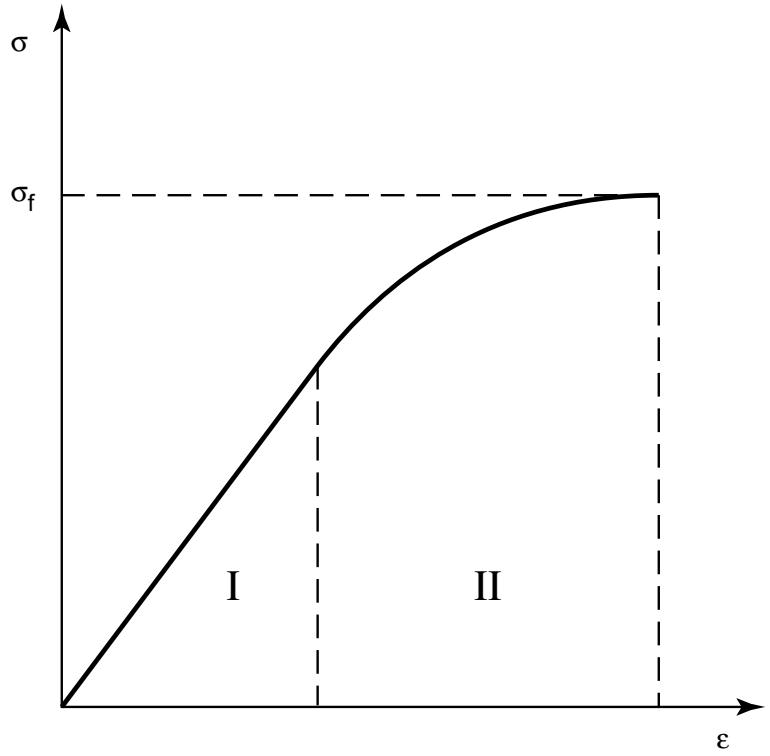

Figure 1. Schematic illustration of the failure of a brittle rod. In region I, linear elasticity is applicable. In region II, damage is occurring and there is irreversible deformation of the rod.

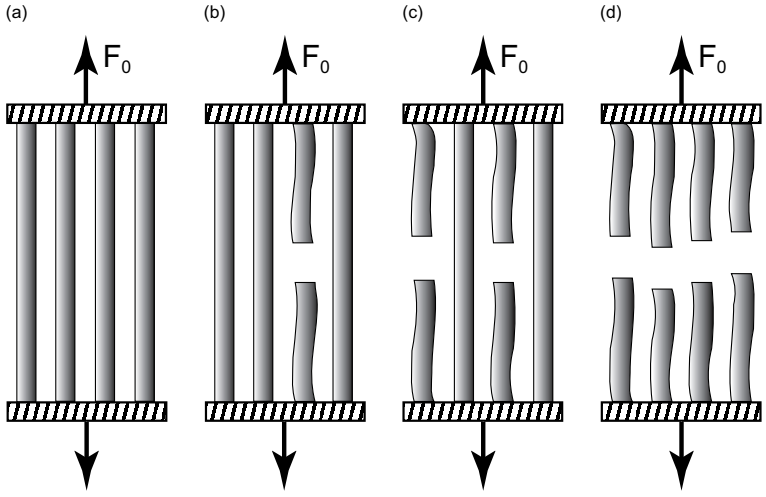

Figure 2. Schematic illustration of the failure of a fiber-bundle with uniform load sharing. (a) Each of the fibers carries one-quarter of the load F_0. (b) One fiber has failed and each remaining fiber carries one-third of the load F_0. Two fibers have failed and each remaining fiber carries one-half of the load F_0. (d) All four fibers have failed and no load is carried.

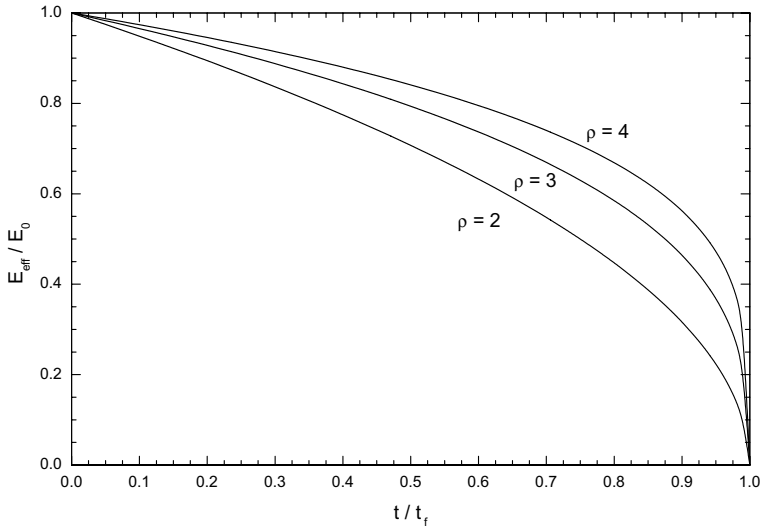

Figure 3. Dependence of the ratio of the effective Young's modulus E_{eff} to the Young's modulus of the undamaged material E_0 on the time to failure t/t_f for $\rho = 2, 3$, and 4 from (2.17). A constant force has been applied to the rod at $t = 0$ and failure occurs at $t = t_f$.

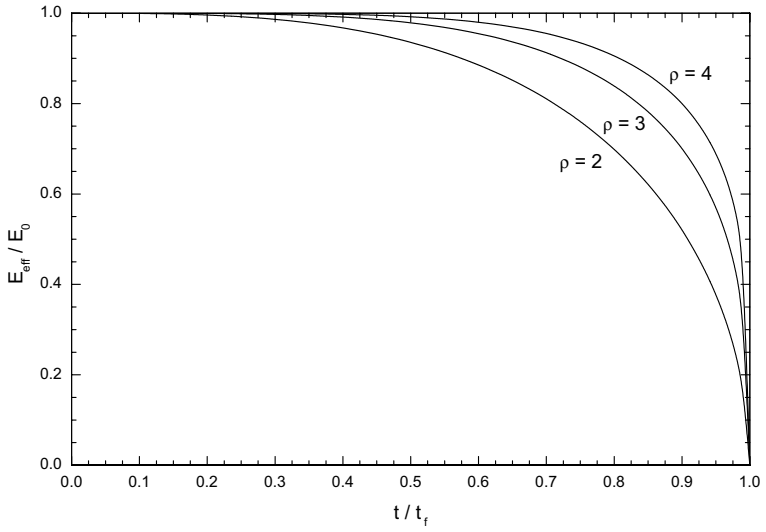

Figure 4. Dependence of the ratio of the effective Young's modulus E_{eff} to the Young's modulus of the undamaged material E_0 on the time to failure t/t_f for $\rho = 2, 3$, and 4 from (5.12). The force on the rod is a linear increasing function of time starting at $t = 0$, failure of the rod occurs at $t = t_f$

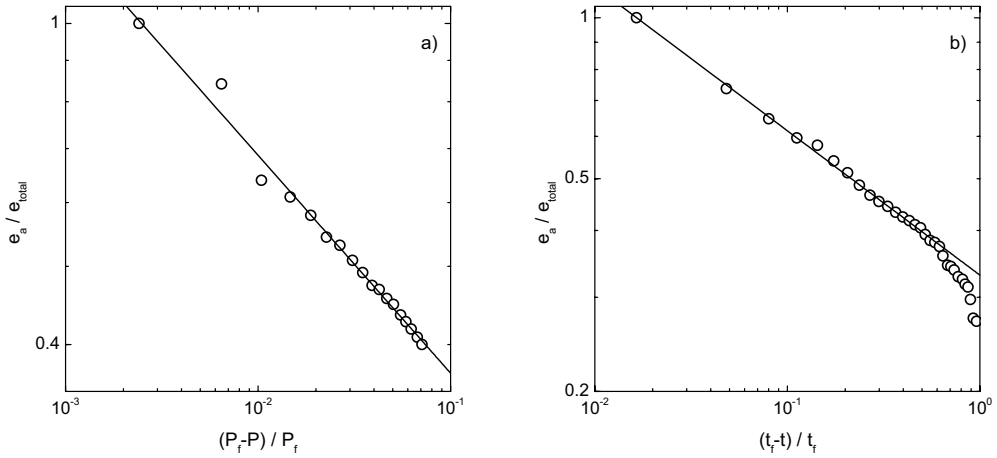

Figure 5. (a) Cumulative acoustic energy emissions $e_a(t)$ divided by the total acoustic energy emissions $e_{\rm tot}$ at the time of rupture $(t = t_f)$ as a function of $(P_f - P)/P_f$ where P is the applied pressure difference across the failing panel of chipboard and P_f is the pressure difference when the board fails. The applied pressure difference across the panel increased linearly with time in accordance with (5.1). The straight-line correlation is with $e_a \propto (1 - t/t_f)^{-0.27}$. (b) Cumulative acoustic energy emissions $e_a(t)$ at time t divided by the total acoustic energy emissions $e_{\rm tot}$ at the time of rupture $(t = t_f)$ as a function of $(1 - t/t_f)$. A constant pressure difference was applied at $t = 0$. The straight-line correlation is with $e_a \propto (1 - t/t_f)^{-0.27}$ (Guarino et al. 1998, 1999).

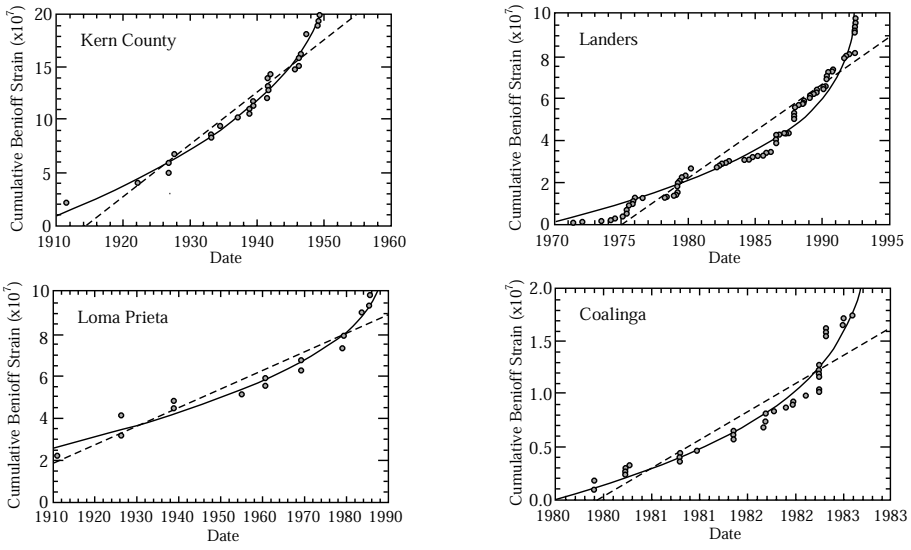

Figure 6. Power-law increase in the cumulative Benioff strain prior to four major earthquakes in California (Bowman et al. 1998). Each of the four examples has been correlated (solid line) with the power-law relation given in (7.2). The dashed straight lines represent a best-fit constant rate of seismicity.